Random Undersampling Wireless EEG Measurement Device using a Small TEG

Takuya Miyata, Daisuke Kanemoto*, and Tetsuya Hirose
Graduate School of Engineering, Osaka University, Suita, Japan
*dkanemoto@eei.eng.osaka-u.ac.jp

***Abstract*—The realization of a compact wireless electroencephalogram (EEG) measurement device that can be used in daily life without concern for power consumption has garnered considerable attention. Thus, wireless EEG measurement devices with energy harvesting have been proposed, but there have been issues with harvester size and power output. In this study, we proposed and implemented a wireless EEG measurement device using compressed sensing, utilizing random undersampling and only a 40 mm×40 mm small thermoelectric generator (TEG) as the power source. The results of the 4x compression experiment revealed a reduction in the power of the microcontroller from 345 μW to 97 μW at 3.3 V. This implies that a wireless EEG measurement device can operate well with a small TEG, even though the reconstructed signal is not inferior to the original signal, in which the average normalized mean square error is approximately 0.24.**

***Index Terms*—electroencephalogram, compressed sensing, thermoelectric generator, random undersampling**

I. Introduction

Electroencephalogram (EEG) signals are important healthcare biometric signals used to reveal signs of brain diseases [1], [2]. Moreover, brain–machine and brain–computer interfaces are being studied to make EEG a promising tool for recognizing user intentions and communicating with external devices [3], [4]. Therefore, wireless EEG measurement devices are being developed to enable easy sensing of EEG signals in daily life. There are numerous wireless EEG devices that are powered by a battery [5]. To realize EEG measurements intended for long-term operation, a large battery must be installed, which is heavy and difficult to use. Therefore, many researchers are working on wireless EEG measurement devices that can operate for long periods of time without the need for batteries or low power output batteries using energy harvesters as the power source.

For instance, an EEG measurement device that utilizes energy from wirelessly transmitted radio waves has been proposed [6]. However, the authors concluded that this design is not robust, because it can only be used near the power source of the antenna. Another study reported a wearable headband with integrated printed active electrodes powered by a flexible solar panel energy harvester [7]. Although the power generated is high and the small harvester is stable for circuit operations, it is not suitable for general use since a significant amount of light is required to generate electricity. Conversely, wireless EEG measurement devices that use thermoelectric generators (TEGs) have garnered attention. TEGs are energy harvesters that can generate electricity from the heat of the human body. To the best of the authors' knowledge, TEG-based EEG measurement device was first reported in [8]. However, its low power output necessitated the use of multiple TEGs to operate measurement devices; 10 TEGs were required in the TEG-based device [8], making the device heavy and unsuitable for daily use.

Therefore, it would be better if the EEG measurement device could work with only a small TEG. This would require a significant reduction in the power consumption. In this study, we focused on compressed sensing (CS) [9], which simultaneously compresses and senses data to reduce the amount of information handled by hardware, thereby realizing the low power consumption of circuits [10]–[12]. Furthermore, we designed and implemented a CS system using random undersampling, which has been discussed to be effective in previous studies (e.g. [13]), and demonstrated the effectiveness of the combination of CS and a small TEG through experiments.

This paper is organized as follows. Section II briefly described the CS theory and advantages of random undersampling in the measurement device. Section III describes the developed system combining a small TEG and CS. In Section IV, implemented system and measurement results with actual EEG signals are shown. Section V presents the conclusions of this study.

II. Basic CS Theory and Advantage of Implementation with Random Undersampling

CS theory is utilized to resolve the problem of obtaining a signal vector $\mathbf{x} \in \mathbb{R}^N$ of size N, which is k-sparse in some basis matrix $\Psi \in \mathbb{R}^{N\times P}$. k-sparse means that only k $(<< P)$ elements of the coefficient vector $\mathbf{s} \in \mathbb{R}^P$, which are used to show that $\mathbf{x} = \Psi\ \mathbf{s}$, are nonzero. Using CS, we can obtain a compressed signal $\mathbf{y} = \Phi\ \mathbf{x}$, where Φ is an $M \times N$ measurement matrix. The compressed signal vector $\mathbf{y} \in \mathbb{R}^M$ is expressed as follows:

$$\mathbf{y} = \mathbf{\Phi x} = \mathbf{\Phi \Psi s}. \tag{1}$$

In this study, compression ratio (CR) was defined as $CR = \frac{N}{M}$. Vector $\mathbf{s}$ is sparse, and there are many zero elements. The length of $\mathbf{y}$ is significantly smaller than that of $\mathbf{s}$. Therefore,

This work was supported by JSPS KAKENHI Grant Number JP21H03410. This paper is based on results obtained from a project, JPNP20004, subsidized by the New Energy and Industrial Technology Development Organization (NEDO).

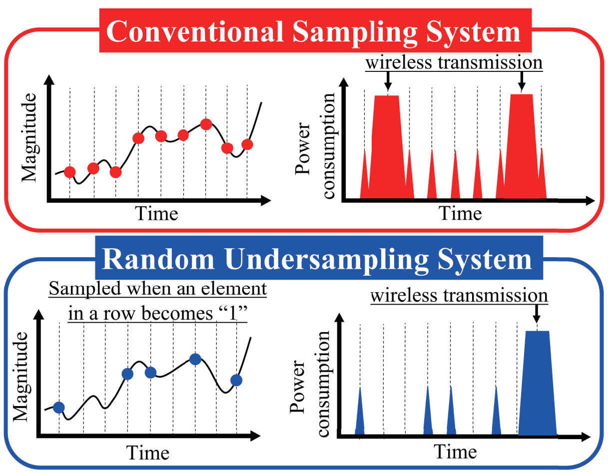

Fig. 1. Comparison of power consumption required for conventional sampling operation and when using random undersampling as CS.

to find $\mathbf{s}$ and thereafter $\mathbf{x}$ from $\mathbf{y}$, the CS problem algorithms are solved [14], [15].

The measurement matrix must be designed considering the hardware components. In this study, random undersampling was used to realize the measurement matrix. The measurement matrix representing random undersampling comprises of one "1" per row with all other "0" [16], as follows:

$$\mathbf{\Phi}_{RU} = \begin{pmatrix} 1 & 0 & 0 & 0 & 0 & \dots & 0 \\ 0 & 0 & 1 & 0 & 0 & \dots & 0 \\ 0 & 0 & 0 & 1 & 0 & \dots & 0 \\ \vdots & \vdots & \vdots & \vdots & \vdots & \ddots & \vdots \\ 0 & 0 & 0 & 0 & 0 & \dots & 1 \end{pmatrix}. \tag{2}$$

To realize $\mathbf{\Phi}_{RU}$ by an A/D converter, sampling is performed when each element of the measurement matrix is "1" [17].

Figure 1 shows a conceptual diagram of the operation and power consumption of the system implementation for equally spaced conventional sampling and random undersampling operations. Conventional sampling requires the continuous operation of the analog-to-digital converter (ADC) and sampled data management circuit, whereas random undersampling can reduce the number of circuit operations because it can achieve unequal spacing and a small number of sampling cycles. In addition, random undersampling reduces the amount of data to be transferred, thereby reducing communication power consumption. A device that operates with only a small TEG can be designed by utilizing these low-power effects.

III. Concept of Designed Device Utilizing Random Undersampling with a Small TEG as Power Supply

A. Overview of System

Figure 2 shows the overall diagram of the designed system. The system comprises three units. The power generation unit comprises a TEG and DC–DC converter. The sensing unit, which operates on the power from the power generator unit, acquires compressed EEG signals via random undersampling

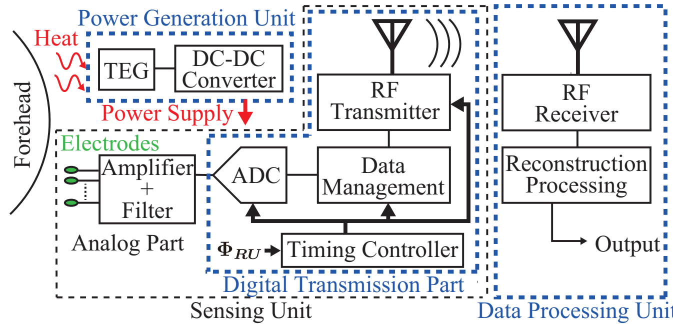

Fig. 2. Concept of our designed EEG measurement system. There are three major units: power generation, sensing, and data processing units. In this study, we have implemented a power generation unit, a digital transmission part as the main power consumption part in the sensing unit, and data processing unit.

and transmits them wirelessly. Finally, the data processing unit receives compressed signals and reconstructs them to achieve the EEG signals.

B. Power Generation Unit

When electricity is generated from the difference between body heat from the forehead and ambient temperature, as in this case, the voltage obtained from the TEG is low to the extent of several tens of millivolts, because the temperature difference is low to the extent of a few degrees. Therefore, a DC–DC converter was used to boost the voltage to supply power to the sensing unit. An important point is that if the power consumption of the sensing unit is high, the output of the DC–DC converter will decrease, and it will not operate. Therefore, it is important to reduce the power consumption of sensing units.

C. Sensing Unit

The sensing unit has two parts: analog part with electrodes, amplifiers, and filters, and a digital transmission part to digitize EEG signals, manage digital data, and transmit data wirelessly. The two popular methods for CS are the analog CS encoder method in analog part, and digital CS encoder method in the digital transmission part (e.g. [18]–[20]). Although they differ in domain, they require computation in either the analog or digital domain. However, our proposed system employs random undersampling, which allows sampling while thinning out the signal, eliminating the need for additional hardware, and making it suitable for research goals for low power consumption. In the proposed sensing unit, based on Φ_{RU}, a timing controller circuit is used to realize the intermittent operation of the ADC, data management, and RF transmitter. When considering the sensing unit as a whole, most of the power consumption is consumed by the A/D converter, digital data management, and wireless communication [21], [22]. In this study, we implemented a digital transmission part, which shows a signal chain after A/D converter to confirm whether device in proposed system can be operated with a small TEG.

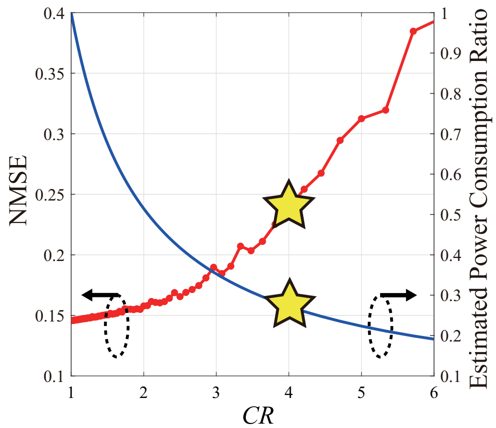

Fig. 3. NMSE (simulation results) and estimated power consumption ratio (theoretical results) when *CR* is varied. In this design, it was found that setting *CR* = 4 produced a well-balanced design.

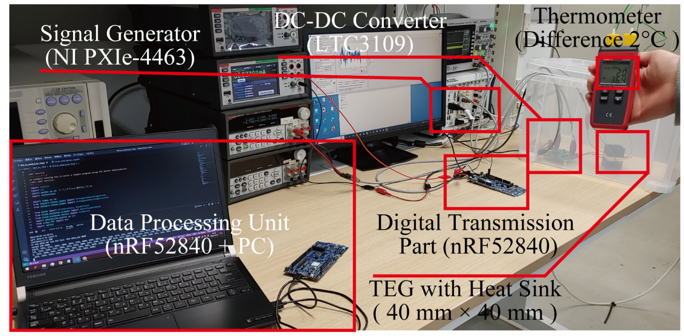

Fig. 4. Verification environment. We observe from the thermometer that a temperature difference of approximately 2 °C was obtained on both sides of the TEG for power generation.

D. Data Processing Unit

The compressed signals transmitted from the sensing unit were reconstructed in the data processing unit. The reconstruction process is performed by an external computer; therefore, there are no restrictions on power consumption, and it can handle heavy computation loads such as CS reconstruction algorithm. The measurement matrix used in the data processing unit is the same Φ_{RS} as in the sensing unit.

IV. Implementation and Evaluation Results

A. Implementation

This section describes the system implemented in Figure 2. CP85438 (CUI Devices) with a heat sink was used as the TEG block in the power generation unit. The size of the TEG was 40 mm $\times$ 40 mm, and LTC3109 [23] from Analog Devices was used as the DC–DC converter. In this design, the LTC3109 implemented board (DC1664A [24]) was used for actual implementation. LTC3109 is capable of functioning with input voltages as low as 30 mV from the TEG. The power obtained from LTC3109 is consumed by the microcontroller in the digital transmission part of the sensing unit. The microcontroller that we selected was nRF52840 from Nordic Semiconductor, and the nRF52840-dk (implemented board) was utilized for this system design. Information on Φ_{RS} was used as the timing controller in the microcontroller to realize random undersampling and intermittent operation of the data management block and RF transmitter. Bluetooth Low Energy (BLE) 5, which is expected to operate with low power consumption, is used for RF transmission. In this system, data packets are organized as follows to check for data loss and efficient communication: A 2-byte counter is inserted at the beginning of the data. The data were converted from 100 12-bit measurements into 150 bytes. In other words, 152-byte packet was passed to the BLE module in one communication. A standard PC (Intel i5 8G RAM) was used for the reconstruction processing. The orthogonal matching pursuit algorithm, a commonly used CS reconstruction algorithm, was implemented using Python3. Discrete cosine transform, often used as a basis, was used for reconstruction.

CR determination is important for implementing a CS system. *CR* can be determined based on the relationship between the reconstruction accuracy and low power consumption achieved by compression. To discuss the reconstruction accuracy, the index of normalized mean square error (NMSE), which indicates the reconstruction error, is utilized as follows:

$$\mathrm{NMSE} = \frac{\|\mathbf{x} - \hat{\mathbf{x}}\|_2^2}{\|\mathbf{x}\|_2^2} \tag{3}$$

where $\mathbf{x}$ and $\hat{\mathbf{x}}$ denote the original and reconstructed EEG signals, respectively. In contrast, we estimated the amount of power consumption reduction compared to the uncompressed power consumption, assuming that the current consumption, except the base current consumption of nRF52840, is inversely proportional to *CR*. Figure 3 shows graphs of the simulated NMSE and estimated power consumption ratio when *CR* is varied. It can be observed that the estimated power consumption ratio can be reduced as *CR* increases, but the NMSE worsens. Incidentally, the reason why NMSE does not become zero when *CR* = 1 is that k used in the reconstruction has a finite value of 20, which is not a problem in principle. From these results, we determined that *CR* is 4, which is better for a well-balanced design (NMSE = 0.23, estimated power consumption ratio = 0.27).

B. Evaluation Results

This study aimed to demonstrate that the digital transmission part of the sensing unit can be operated using only a small TEG utilizing random undersampling. Therefore, we tested the operation of the digital transmission part with EEG signals that were properly amplified to the full-scale range of the ADC. We used the National Instrument PXIe-4463 as a signal source, which is capable of outputting EEG signals from a healthy student in his 20s, sampled at 256 Hz from 16 electrodes arranged according to the 10–20 electrode positioning system [25]. The EEG obtained from the FP1 electrode was used for validation. In this study, a single frame comprised of 800 points, corresponding to 3.125 s.

TABLE I
COMPARISON OF THE DESIGNED EEG MEASUREMENT DEVICE WITH OTHER DEVICES UTILIZING VARIOUS ENERGY HARVESTERS.

	This work	A.Dementyev et al. [6]	J.W.Matiko et al. [7]	T.Torfs et al. [8]
Power Consumption [μ W]	**97**(1)	432(2)	N/A	495(1)
Sampling Rate [Hz] (Resolution [bit])	**256**(3) **(12)**	63 (10)	128 (10 (estimation))	256 (12)
Energy Harvester (Harvester Size)	**TEG**(4) **(40 mm×40 mm)**	RF antenna (N/A)	Solar panel (37mm × 84mm × 4)	TEG (16 mm × 40mm × 10)
EEG Channel Number	**1**	1 + DRL	2 +DRL	2

(1) ADC, Data Management, and Wireless transmitter (digital transmission part)
(2) EEGWISP part
(3) Sampling rate after reconstruction
(4) No wind and a temperature difference of approximately only 2°C.

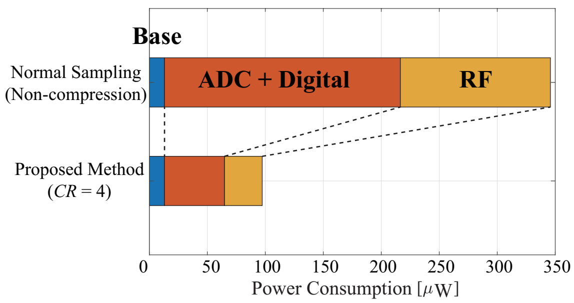

Fig. 5. Experimental results of power consumption. The proposed method reduces power consumption by 28% with *CR* = 4.

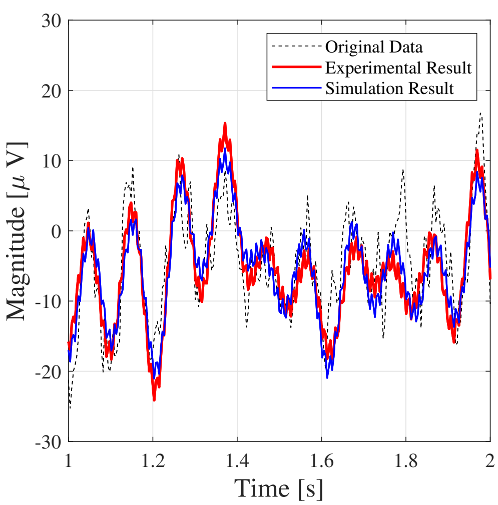

Fig. 6. Zoom view of the waveform from 1.0 to 2.0 s. There is no significant difference between the result of the simulation and the experimental result.

Figure 4 shows the verification environment. When power is generated with a TEG, it is necessary to achieve a temperature difference. In this verification, we assumed a room temperature of 26°C against a forehead temperature of 36°C, and realized an environment in which a temperature difference of approximately 2°C could be provided to the TEG, even with thermal resistance (heat sink: TEG = 8:2). The TEG and DC–DC converter were placed in a plastic case to prevent wind inflow and ensure an accurate and stable evaluation environment. A Keithley DMM6500 digital multimeter was used to comprehensively measure the microcontroller current consumption. Figure 5 shows the power consumption for normal sampling and the proposed method (*CR* = 4). The microcontroller benefitted from compression, reducing the power consumption by a factor of approximately 1/4. Therefore, 97 μW at 3.3 V can be achieved by utilizing random undersampling, although power consumption due to non-compression was 345 μW at 3.3 V.

Figure 6 shows the reconstructed single-frame data obtained from the simulations and experiments for 1 to 2 s of the original signal. The results show that there is almost no difference between the experimental and software simulation results. There was also no significant difference between the original and reconstructed waveforms, indicating that a clean reconstructed waveform could be obtained even when *CR* was increased by a factor of 4 by random undersampling. The average NMSE was 0.24 for the 100 frames measured, which was almost in line with the simulation.

Thanks to 4x compression, the whole system works well even when using the small TEG as a power source, however, it was also confirmed that it does not operate due to insufficient power supply when the system is operated uncompressed by experiment.

C. Comparison

Table I compares the characteristics of the EEG devices used for this verification with those of other devices that use energy harvesters. First, our device consumes the least amount of power, although the sampling rate of the reconstruction data and ADC resolution are similar to those of the commonly used EEG devices. Unlike solar energy, the low power generation of the TEG is considered to be a drawback. However, the power consumption of the device designed in this study is extremely low. Hence, the low power obtained from the small 40 mm × 40 mm TEG is sufficient for device operation.

V. CONCLUSION

In this study, we designed a wireless EEG measurement device that operates based on the CS theory with random undersampling and showed that it can be powered by a small TEG of 40 × 40 mm with low power consumption. The power consumption is reduced to 97 μ W by selecting *CR* = 4. The average NMSE of the acquired EEG signals over 100 frames was 0.24, which is close to the simulation result of 0.23, confirming the effectiveness of the actual device. This study demonstrated new possibilities for compact EEG measurement devices by combining CS and energy-harvesting technologies.

References

[1] H. R. Mohseni, A. Maghsoudi, and M. B. Shamsollahi, "Seizure detection in EEG signals: A comparison of different approaches," in *in Proc. Int. Conf. IEEE Eng. Med. Biol. Soc.*, Mar. 2006, pp. 6724–6727.

[2] T. Musha, H. Matsuzaki, Y. Kobayashi, Y. Okamoto, M. Tanaka, and T. Asada, "EEG markers for characterizing anomalous activities of cerebral neurons in NAT (Neuronal Activity Topography) method," *IEEE Trans. Biomed. Eng.*, vol. 60, no. 8, pp. 2332–2338, Apr. 2013.

[3] J.-H. Jeong, K.-H. Shim, D.-J. Kim, and S.-W. Lee, "Brain-controlled robotic arm system based on multi-directional CNN-BiLSTM network using EEG signals," *IEEE Trans. Neural Syst. Rehabil. Eng.*, vol. 28, no. 5, pp. 1226–1238, Mar. 2020.

[4] E. Yin, Z. Zhou, J. Jiang, Y. Yu, and D. Hu, "A dynamically optimized SSVEP brain–computer interface BCI speller," *IEEE Trans. Biomed. Eng*, vol. 62, no. 6, pp. 1447–1456, Apr. 2015.

[5] L. Brown, J. van de Molengraft, R. F. Yazicioglu, T. Torfs, J. Penders, and C. Van Hoof, "A low-power, wireless, 8-channel EEG monitoring headset," in *Proc. Annu. Int. Conf. IEEE Eng. Med. Biol*, Aug. 2010, pp. 4197–4200.

[6] A. Dementyev and J. R. Smith, "A wearable uhf rfid-based EEG system," in *Proc. IEEE Int. Conf. RFID*, Apr. 2013, pp. 1–7.

[7] J. W. Matiko, Y. Wei, R. Torah, N. Grabham, G. Paul, S. Beeby, and J. Tudor, "Wearable EEG headband using printed electrodes and powered by energy harvesting for emotion monitoring in ambient assisted living," *Smart Mater. Struct.*, vol. 24, no. 12, pp. 125 028–125 038, Nov. 2015.

[8] T. Torfs, V. Leonov, R. F. Yazicioglu, P. Merken, C. Van Hoof, R. J. Vullers, and B. Gyselinckx, "Wearable autonomous wireless electro-encephalography system fully powered by human body heat," in *SENSORS, 2008 IEEE*, Dec. 2008, pp. 1269–1272.

[9] D. L. Donoho, "Compressed sensing," *IEEE Trans. Inf. Theory*, vol. 52, pp. 1289–1306, Apr. 2006.

[10] S. Aviyente, "Compressed sensing framework for EEG compression," in *Proc. IEEE/SP 14th Workshop Stat. Signal Process.*, Aug. 2007, pp. 181–184.

[11] Y. Dai, X. Wang, X. Li, and Y. Tan, "Sparse EEG compressive sensing for web-enabled person identification," *Measurement*, vol. 74, pp. 11–20, Oct. 2015.

[12] F. Chen, A. P. Chandrakasan, and V. Stojanović, "A signal-agnostic compressed sensing acquisition system for wireless and implantable sensors," in *Proc. IEEE CICC 2010*, Sep. 2010, pp. 1–4.

[13] D. Kanemoto, S. Katsumata, M. Aihara, and M. Ohki, "Framework of applying independent component analysis after compressed sensing for electroencephalogram signals," in *Proc. IEEE Biomed. Circuits Syst. Conf. (BioCAS)*, Oct. 2018, pp. 1–4.

[14] Z. Zhang, T.-P. Jung, S. Makeig, and B. D. Rao, "Compressed sensing of EEG for wireless telemonitoring with low energy consumption and inexpensive hardware," *IEEE Trans. Biomed. Eng.*, vol. 60, no. 1, pp. 221–224, Jan. 2013.

[15] J. A. Tropp and A. C. Gilbert, "Signal recovery from random measurements via orthogonal matching pursuit," *IEEE Trans. Inf. Theory*, vol. 53, no. 12, pp. 4655–4666, Dec. 2007.

[16] Y. Okabe, D. Kanemoto, O. Maida, and T. Hirose, "Compressed sensing EEG measurement technique with normally distributed sampling series," *IEICE Trans. Fundamentals*, vol. E105-A, no. 10, pp. 1429–1433, Oct. 2022.

[17] M. Trakimas, R. D'Angelo, S. Aeron, T. Hancock, and S. Sonkusale, "A compressed sensing analog-to-information converter with edge-triggered SAR ADC core," *IEEE Trans. Circuits Syst. I, Reg. Papers*, vol. 60, no. 5, pp. 1135–1148, Apr. 2013.

[18] F. Chen, A. P. Chandrakasan, and V. M. Stojanovic, "Design and analysis of a hardware-efficient compressed sensing architecture for data compression in wireless sensors," *IEEE J. Solid-State Circuits*, vol. 47, no. 3, pp. 744–756, Mar. 2012.

[19] H. Qian, X. Song, D. Li, and Z. Wang, "Generalized analog-to-information converter with analysis sparse prior," *IEEE Trans. Circuits Syst. I, Reg. Papers*, vol. 68, no. 9, pp. 3574–3586, Jun. 2021.

[20] D. Valencia, J. Thies, and A. Alimohammad, "Frameworks for efficient brain-computer interfacing," *IEEE Trans. Biomed. Circuits Syst.*, vol. 13, no. 6, pp. 1714–1722, Oct. 2019.

[21] J. Van Assche and G. Gielen, "Power efficiency comparison of event-driven and fixed-rate signal conversion and compression for biomedical applications," *IEEE Trans. Biomed. Circuits Syst.*, vol. 14, no. 4, pp. 746–756, Jul. 2020.

[22] S. Katsumata, D. Kanemoto, and M. Ohki, "Applying outlier detection and independent component analysis for compressed sensing EEG measurement framework," *Proc. IEEE Biomed. Circuits Syst. Conf. (BioCAS)*, pp. 1–4, Oct. 2019.

[23] Analog Devices, *Auto-polarity, ultralow voltage step-Up converter and power manager*, LTC3109 datasheet, Aug. 2013, [Rev. B].

[24] ——, *LTC3109EUF auto-polarity, ultralow voltage step-up converter and power manager*, DC1664A manual, Oct. 2010.

[25] R. Oostenveld and P. Praamstra, "The five percent electrode system for high-resolution EEG and ERP measurements," *Clin. Neurophysiol.*, vol. 112, no. 4, pp. 713–719, Apr. 2001.